Miscibility Behavior of Ternary Poly(methyl methacrylate)/Poly(ethyl methacrylate)/Poly(*p*-vinylphenol) Blends

J. A. Pomposo, E. Calahorra, I. Eguiazabal, and M. Cortazar*

Departamento de Ciencia y Tecnología de Polímeros, Facultad de Ciencias Químicas de San Sebastián, P.O. Box 1072, San Sebastián, Spain

Received August 6, 1992; Revised Manuscript Received December 21, 1992

ABSTRACT: The phase behavior of ternary blends consisting of poly(methyl methacrylate) (PMMA), poly(ethyl methacrylate) (PEMA), and poly(*p*-vinylphenol) (PVPh) was investigated by differential scanning calorimetry (DSC) and scanning electron microscopy (SEM). The assessment of miscibility was based mainly on the presence of a single glass transition. In this ternary blend where PVPh is miscible with each of the other components, more than 60 wt % PVPh was required to cause miscibility between PMMA and PEMA. Based on the glass transition temperature data, a ternary phase diagram was constructed. The miscibility behavior of the ternary PMMA/PEMA/PVPh blends as well as of the PMMA/PEMA/poly(vinylidene fluoride) (PVF_2) and PMMA/PEMA/poly(styrene-*co*-acrylonitrile) (SAN) systems was rationalized using the spinodal condition and the Flory–Huggins theory in an attempt to test the validity of this theoretical approach for these systems. Values of the interaction energy between PMMA and PEMA, which correlate quite well between them, were derived from the experimental ternary diagrams. A prediction of the miscibility behavior for ternary PMMA/PEMA/poly(styrene-*co*-maleic anhydride) (SMA) blends was attempted based on these values.

Introduction

It is well known that miscibility between polymers often results if specific interactions are present between different structures of the polymers that constitute the mixture. In particular, polymers containing hydroxyl groups are often miscible or partially miscible with ester-containing polymers.[1,2] Therefore, it is not surprising that poly(*p*-vinylphenol) (PVPh) shows miscibility with some acrylic polymers. The miscibility of the poly(methyl methacrylate)/poly(*p*-vinylphenol) (PMMA/PVPh) and poly(ethyl methacrylate)/poly(*p*-vinylphenol) (PEMA/PVPh) systems has been previously studied by Goh and Siow,[3] and they observed miscibility in all its compositional range. Coleman et al.[4] claim these systems are miscible as a consequence of intermolecular hydrogen-bonding interactions, which have been detected by Fourier transform infrared spectroscopy (FTIR).

Although PMMA and PEMA are both miscible with PVPh, the two methacrylate polymers are immiscible with each other. Due to the industrial importance of overcoming property deficiences of immiscible blends, it seems interesting to explore the possibility of rendering these two polymers miscible using PVPh as a common solvent. The addition of a suitable third polymer to solubilize PMMA and PEMA has already been reported by several authors. Kwei et al.[5] used poly(vinylidene fluoride) to compatibilize them. Goh and Siow[6,7] have reported the miscibility behavior of ternary PMMA/PEMA/SAN and PMMA/PEMA/poly(α-methylstyrene-*co*-acrylonitrile) (MSAN) blends. In this paper, the miscibility of ternary PMMA/PEMA/PVPh blends will be studied.

Efforts to rationalize the equilibrium phase behavior of ternary polymer systems have been recently made in the literature.[8-11] The exact calculation of the phase diagram is very difficult indeed because no analytical expression for the binodal (coexistence) curve exists, so the spinodal condition with the Flory–Huggins theory has been used to reproduce the experimental miscibility boundary.[12,13] The free energy of mixing (per unit volume) in a monodisperse ternary polymer blend is given by[14]

$$\Delta G_m/V = RT\left(\frac{\phi_1 \ln \phi_1}{V_1} + \frac{\phi_2 \ln \phi_2}{V_2} + \frac{\phi_3 \ln \phi_3}{V_3}\right) + B_{12}\phi_1\phi_2 + B_{13}\phi_1\phi_3 + B_{23}\phi_2\phi_3 \quad (1)$$

where V is the mixture volume, V_i is the molar volume of component i, and B_{ij} is the interaction energy density related to the enthalpic interactions between i and j. For blends composed of polydisperse polymers, number-average molecular weights can be used in eq 1 to compute molar volumes, and if strong specific interactions are involved (e.g., hydrogen bonds), a dependence on composition of the B_{ij} parameter can be expected.[15] Values of the interaction energy densities can be experimentally determined by several common techniques (e.g., melting-point depression, vapor sorption, analogue calorimetry, copolymer phase behavior, etc.) or obtained from the literature, when available. Thus, if the pertinent B_{ij} coefficients are known, the spinodal curve of the ternary blend can be determined from eq 1 and the following condition:[12]

$$\left[\frac{\partial^2(\Delta G_m/V)}{\partial \phi_1^2}\right]_{T,P}\left[\frac{\partial^2(\Delta G_m/V)}{\partial \phi_2^2}\right]_{T,P} - \left[\frac{\partial^2(\Delta G_m/V)}{\partial \phi_1 \partial \phi_2}\right]_{T,P}^2 = 0 \quad (2)$$

The spinodal curve defines the boundary between unstable and metastable mixtures. Thermodynamically, when the left-hand side of eq 2 is negative, the system always separates into different phases.

On the other hand, quantitative information about binary interaction energies can be extracted from the experimental phase boundary employing eqs 1 and 2. This procedure will be used in this paper to obtain the interaction energy density between PMMA and PEMA.

Experimental Section

The polymers used in this study and some of their characteristics are summarized in Table I.

PMMA/PEMA/PVPh blends were prepared by slowly casting films from methyl ethyl ketone (MEK) solutions, containing

* To whom correspondence should be addressed.

0024-9297/93/2226-2104$04.00/0

Table I
Polymers Used in This Work

polymer	source	mol wt	density (g/cm³)
poly(methyl methacrylate (PMMA)	ICI, Diacom Acrylic	M_w = 108 000[a]	1.17[b]
poly(ethyl methacrylate) (PEMA)	Du Pont (Elvacite 2042)	M_w = 310 000[c]	1.12[b]
poly(*p*-vinylphenol) (PVPh)	Polysciences Inc.	M_w = 30 000[d]	1.15[e]

[a] Determined experimentally in this laboratory by GPC. [b] Source: ref 16. [c] Source: ref 3. [d] Provided by supplier. [e] Source: ref 17.

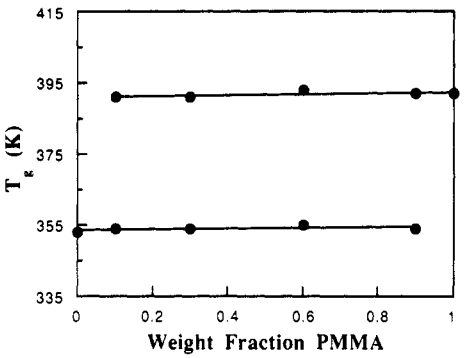

Figure 1. Glass transition temperatures of binary PMMA/PEMA blends as a function of composition.

adequate proportions of each homopolymer. Solvent evaporation was first conducted at room temperature; then, to ensure the complete removal of MEK, the films were dried for 1 day at 353 K in a vacuum oven, heated at 423 K for 3 h, and then slowly cooled to room temperature.

Differential scanning calorimetry (DSC) measurements were conducted with a Perkin-Elmer DSC-2 apparatus equipped with a TADS microcomputer; the apparatus was calibrated with indium. Glass transition measurements were taken as follows: the samples were first heated in the DSC at a heating rate of 40 K/min up to 423 K and maintained 3 min at that temperature to ensure well-defined and reproducible transitions. Glass transition temperatures (T_g) were subsequently recorded at a heating rate of 20 K/min in a second scan. The T_g's were measured at half-height of the corresponding heat capacity jump.

Scanning electron microscopy (SEM) studies on binary and ternary blends were carried out after gold coating of fracture surfaces using a Hitachi S2700 scanning microscope operated at 15 kV.

Heats of mixing for low molecular weight analogues of the corresponding polymers were measured using a Setaram C.80 D flux-type calorimeter. All chemicals used were obtained from Aldrich Chemical Co. and were better than 99% pure. 4-Ethylphenol (EPH) was selected as a model compound of PVPh, whereas methyl pivalate (MPI) and ethyl isobutyrate (EIB) were employed as analogues of PMMA and PEMA, respectively. They were used as received without further purification. The experiments were conducted at 352.2 ± 0.1 K, a temperature above the melting point of EPH (318 K) and below the boiling point of MPI (374 K) and EIB (385 K).

Results and Discussion

Binary Blends. A single, composition-dependent, glass transition temperature was used as a miscibility criterion in this work. DSC analysis of PMMA/PEMA blends shows the presence of two glass transitions, nearly independent of blend composition (Figure 1). This result suggests practically complete immiscibility of PMMA and PEMA, in agreement with previous reports.[5,18]

There are several papers in the literature that estimate the energy of interaction between PMMA and PEMA,

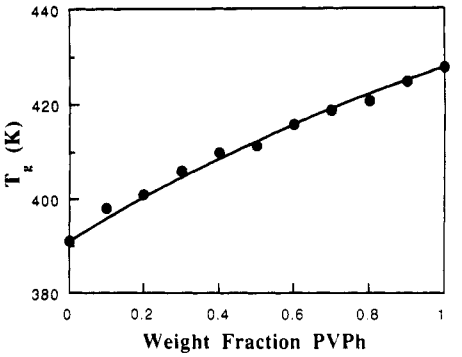

Figure 2. Glass transition temperatures of binary PMMA/PVPh blends as a function of composition.

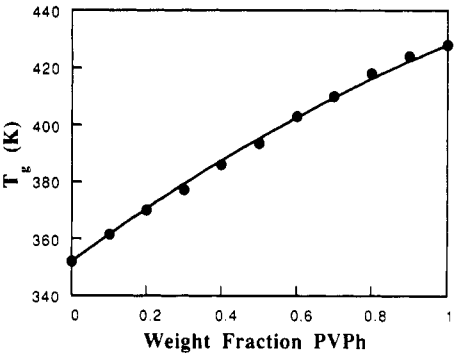

Figure 3. Glass transition temperatures of binary PEMA/PVPh blends as a function of composition.

pointing out the existence of unfavorable weak forces between them, which give rise to an endothermic enthalpy of mixing opposing miscibility. Melting-point depression analysis of the PMMA/PEMA/PVF_2 ternary blend[5] gives an interaction energy density of 0 ± 0.5 cal/cm³. From copolymer miscibility windows[19] a value of +0.13 cal/cm³ is obtained using the Flory–Huggins theory and +0.15 cal/cm³ with the lattice–fluid theory. Finally, the solubility parameter approach[16] gives estimates of the interaction energy density between +0.03 and +0.11 cal/cm³, in agreement with the above values. Interestingly, repulsive interactions slightly larger than that for PMMA/PEMA blends have been found between PMMA and other polymethacrylates. Thus, a value of +0.3 cal/cm³ was obtained for PMMA/poly(phenyl methacrylate) blends and +0.8 cal/cm³ for the system PMMA/poly(cyclohexyl methacrylate).[20]

The T_g–composition curves of PMMA/PVPh and PEMA/PVPh blends have been previously reported,[3] but the PVPh molecular weight employed differs considerably from that used in this work. We have examined the T_g behavior of these systems (Figures 2 and 3) with our own polymer samples to understand the results concerning the ternary blends. In both systems the T_g's are slightly higher than those predicted by the additivity rule.[21]

Some blend compositions were heated in the DSC up to 473 K and then quickly cooled to room temperature. In the next heating run only one T_g was observed, suggesting that the lower critical solution temperature (LCST) cannot be detected in these systems below the decomposition temperature of polymethacrylates. Both the positive deviation from additivity in glass transition temperatures and the absence of a LCST below 473 K suggest the presence of exothermic (favorable) interactions in these systems.[21,22]

To our knowledge, interaction parameters of PMMA/PVPh and PEMA/PVPh blends have not been reported in the literature, so we have employed analogue calorimetry

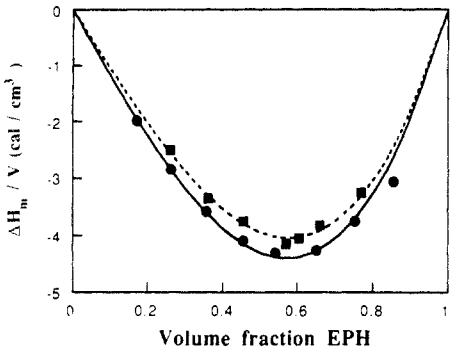

Figure 4. Composition dependence of the heats of mixing for EPH/MPI (■) and EPH/EIB (●) mixtures as low molecular weight models of PVPh/PMMA and PVPh/PEMA blends, respectively. The continuous and dashed lines are computed from eqs 4 and 5 in the text.

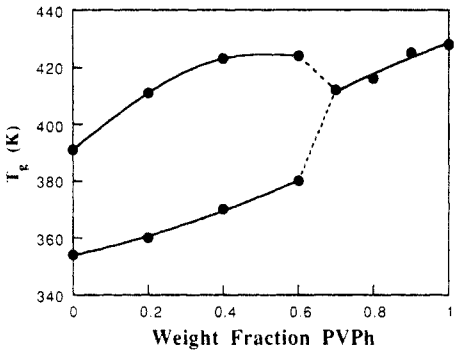

Figure 5. Effect of PVPh on the glass transition behavior of ternary blends containing a PMMA/PEMA ratio of 10/90.

to estimate these parameters that govern blend miscibility. Since the enthalpy of mixing arises from energy changes between nearest-neighbor contacts, the heat of mixing between polymer segments has been found to be almost equivalent to the heat of mixing of the model compounds.[23-25] Although it is known that analogue calorimetry provides only the enthalpic contribution to the interaction energy density (entropic contributions are not taken into account), the B_{ij} parameter so calculated can be used as a first approximation since for several systems it compares reasonably well with those obtained by other techniques such as melting-point depression[26-28] and vapor sorption.[26] Figure 4 shows the composition dependence of the heat of mixing for MPI/EPH and EIB/EPH mixtures as model compounds of PMMA/PVPh and PEMA/PVPh blends, respectively. The interaction energy density is related to the heat of mixing (ΔH_m) by

$$B_{ij} = \frac{\Delta H_m / V}{\phi_i \phi_j} \quad (3)$$

Interaction parameters that depend on the volume fraction of EPH are needed to fit the data, since the experimental curves are both asymmetrical. The following expressions are used, which reproduce adequately the heats of mixing as one can see in Figure 4:

$$B_{EPH/MPI} = -10.53 - 10.47\phi_{EPH} \quad (cal/cm^3) \quad (4)$$

$$B_{EPH/EIB} = -11.96 - 10.49\phi_{EPH} \quad (cal/cm^3) \quad (5)$$

Ternary Blends. Glass transition temperatures were measured for a variety of compositions of the ternary PMMA/PEMA/PVPh blends containing PMMA/PEMA ratios of 10/90, 30/70, 60/40, and 90/10. Figures 5–8 show the effect of PVPh addition on the glass transition behavior

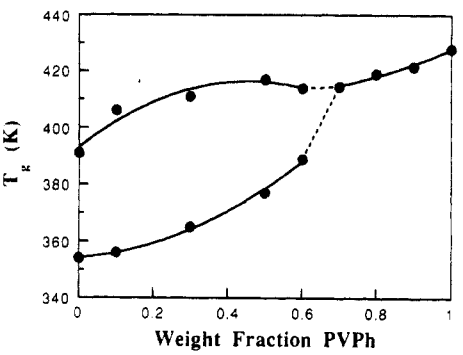

Figure 6. Effect of PVPh on the glass transition behavior of ternary blends containing a PMMA/PEMA ratio of 30/70.

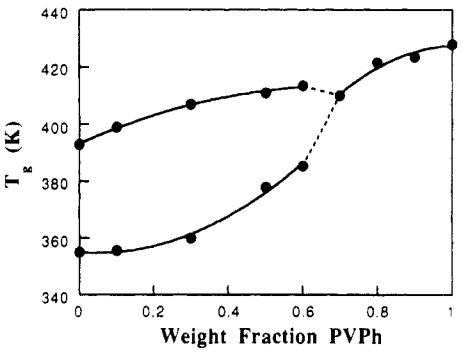

Figure 7. Effect of PVPh on the glass transition behavior of ternary blends containing a PMMA/PEMA ratio of 60/40.

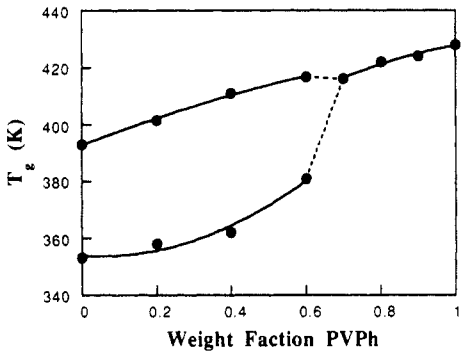

Figure 8. Effect of PVPh on the glass transition behavior of ternary blends containing a PMMA/PEMA ratio of 90/10.

of the ternary blends. Blends containing less than 60 wt % PVPh had two distinct T_g's which appear to correspond to a PMMA-rich phase, containing mostly PMMA and PVPh, and a PEMA-rich phase, containing mostly PEMA and PVPh. T_g values of the PMMA-rich phase are maintained above the value of the additive rule for PMMA and PVPh pure components, whereas T_g values of the PEMA-rich phase are below this rule for PEMA and PVPh pure components. The addition of sufficient PVPh caused the ternary mixture to show a single-T_g behavior. Figures 5–8 show that the miscibility boundary is located between 60 and 70 wt % PVPh in the system, whatever the PMMA/PEMA ratio is.

A simple analysis of the glass transition behavior for the immiscible region can be done supposing that PVPh is distributed in two binary phases, one containing PMMA and PVPh and the other containing PEMA and PVPh. Based on this assumption, proper material balance and T_g–composition curves of each binary blend (Figures 2 and 3) allow us to calculate the higher (or lower) T_g from the experimental lower (or higher) T_g. Figure 9 shows a fair agreement between the experimental and calculated T_g's for the PMMA/PVPh phase. Although this simple

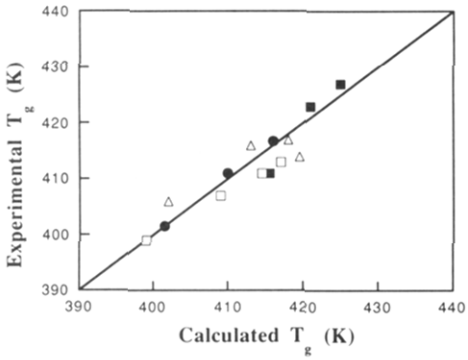

Figure 9. Comparison between the experimental higher T_g of ternary immiscible compositions and the calculated T_g corresponding to a PMMA/PVPh binary phase (see text) for several PMMA/PEMA ratios: (■) 10/90; (△) 30/70; (□) 60/40; (●) 90/10.

Table II
Comparison between the Experimental and Calculated T_g's without Taking into Account the Presence of the Minor Component in the Miscible Ternary Blend[a]

composition, wt %			T_g (K)	
PMMA	PEMA	PVPh	exptl	calcd
3	27	70	412	412
2	18	80	416	417
1	9	90	425	423
9	21	70	414	415
6	14	80	419	420
3	7	90	421	424
27	3	70	416	420
18	2	80	422	423
9	1	90	424	426

[a] Data for miscible ternary blends of PMMA/PEMA (60/40 ratio) were not considered because the amount of the minor component is quite important.

model is able to reproduce experimental trends acceptably, ternary phases instead of binary ones are probably involved. In this sense, we have calculated the T_g of some miscible ternary blends without taking into account the presence of the minor component in the mixture (see Table II). The results show that even a relatively high percentage of the third component (~10 wt %) does not alter considerably the T_g corresponding to the binary blend. Consequently, we cannot ascertain by DSC if binary or ternary phases are involved in the immiscible region of PMMA/PEMA/PVPh blends. This fact prevents us from knowing the composition of the coexisting phases, related to the binodal curve.

Concerning the single-T_g region, this behavior could be due to the formation of a single ternary phase composed of the three polymers of the mixture or to the coexistence of two phases with similar T_g's. However, in the transition region from two T_g's to a single T_g, the T_g's of the two phases are sufficiently apart that a slight increase of the PVPh content would not be expected to produce an overlap of the T_g's of the two phases. On the other hand, it is known that a glass transition broadening could be attributed to composition fluctuations[29] or to an incomplete overlap of the T_g's corresponding to several phases. In our case, the single T_g that emerges with increasing PVPh content is not broader than those of each of the two phases. This behavior suggests that finally PVPh renders the two methacrylate polymers miscible.

Additional information on the subject is provided by scanning electron microscopy (SEM). Figure 10 shows photomicrographs obtained for the PMMA/PEMA (60/40) blend and for the same PMMA/PEMA ratio with the addition of 30% and 70% PVPh. It can be seen that the

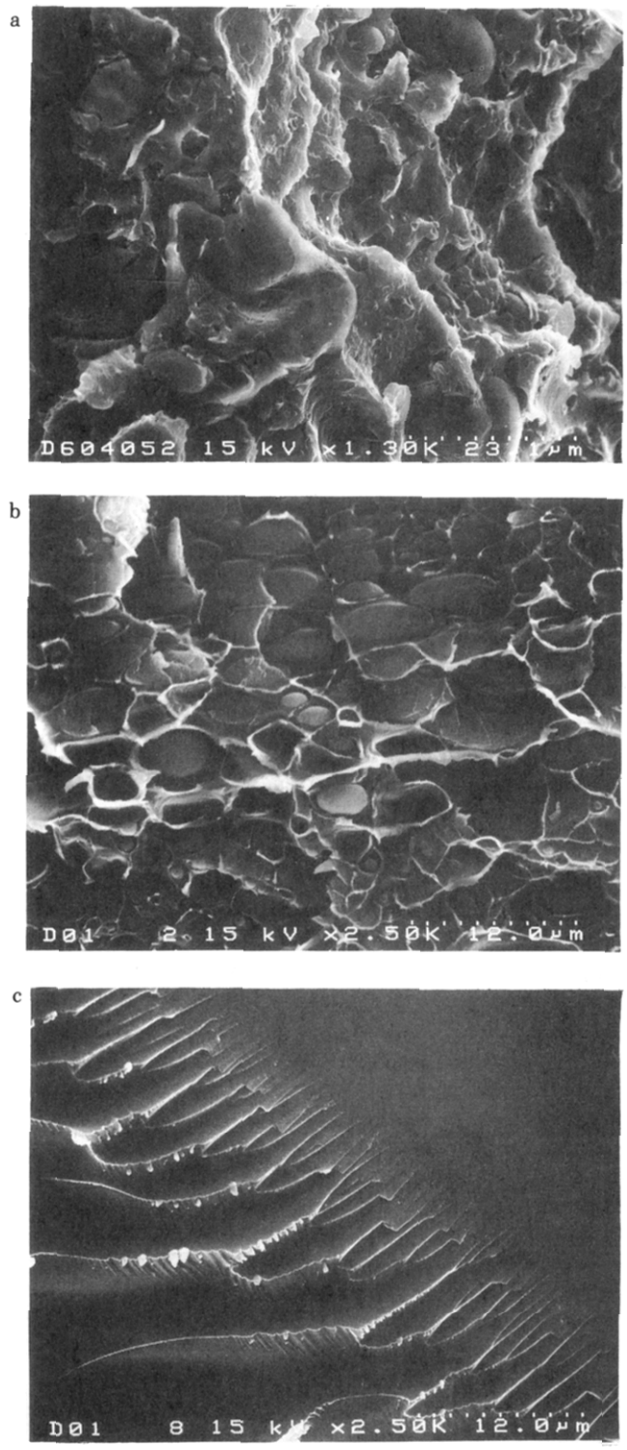

Figure 10. SEM photomicrographs of ternary blends containing a PMMA/PEMA ratio of 60/40 and varying amounts of PVPh: (a, top) 0% PVPh; (b, middle) 30% PVPh; (c, bottom) 70% PVPh.

PMMA/PEMA (60/40) blend (Figure 10a) clearly exhibits phase separation, with a matrix-dispersed phase morphology and a wide size distribution of the dispersed phase. This morphology agrees with the two glass transitions observed by DSC for this PMMA/PEMA blend. The PMMA/PEMA (60/40) blend with 30% PVPh also shows two glass transitions and the corresponding SEM photomicrograph (Figure 10b) phase separation. However, the particle size is smaller than in the absence of PVPh. This result may be attributed to an emulsifying effect of PVPh, similar to that which has been observed in some cases upon the addition of block or graft copolymers to immis-

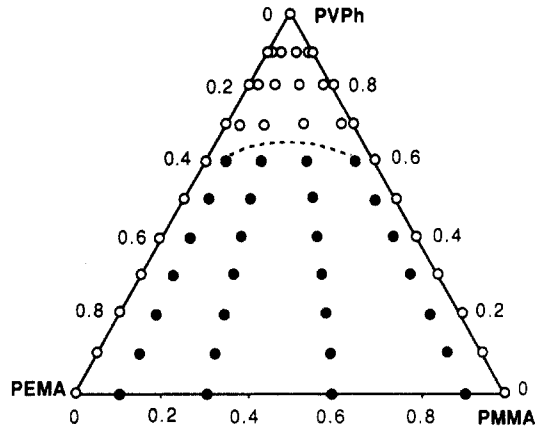

Figure 11. Ternary diagram of the PMMA/PEMA/PVPh system. The open circles represent compositions where a single T_g is observed, and the full circles represent compositions where two glass transitions are observed. The miscibility boundary is denoted by the broken line. (Coordinates in volume fraction.)

cible blends.[30] Finally, Figure 10c is the SEM photomicrograph obtained for the PMMA/PEMA (60/40) blend with 70% PVPh. The DSC thermogram of this blend has a single glass transition, and the SEM photomicrograph clearly indicates the monophasic nature of the blend and the miscibilization of the originally immiscible PMMA/PEMA blend by the addition of PVPh.

The ternary diagram denoting compositions where a single T_g or two T_g's are observed in shown in Figure 11. By comparing our results with those reported in the bibliography for systems where a third component acts a compatibilizer of PMMA and PEMA, we can say that the size of the single-T_g region in Figure 11 is smaller than that showed by the ternary PMMA/PEMA/SAN or PMMA/PEMA/MSAN blends where 40 wt % or even less SAN or MSAN is enough to produce a single T_g.[6,7] For the PMMA/PEMA/PVF_2 system, blends containing 40–70 wt % PVF_2 consist of a single phase, but when the amount of PVF_2 is further increased to 80 wt %, it is not possible to avoid the PVF_2 crystallization by quenching from the melt, so the PVF_2 content in the amorphous state decreases considerably and the mixture appears to contain crystalline regions as well as multiple amorphous phases.[5,31] In a few words, the SAN-related copolymers and PVF_2 are more effective compatibilizers for PMMA and PEMA than PVPh.

A simple way to rationalize these trends is provided by the Flory–Huggins theory[14] extended to the case of three-component polymer mixtures. Let us assume that polymer 1 is miscible with polymers 2 and 3 but that they are immiscible with each other. Then using eqs 1 and 2 the spinodal condition is given explicitly by[32–36]

$$\left(\frac{RT/V_1}{\phi_1}+\frac{RT/V_3}{\phi_3}-2B_{13}\right)\left(\frac{RT/V_2}{\phi_2}+\frac{RT/V_3}{\phi_3}-2B_{23}\right)-\left(\frac{RT/V_3}{\phi_3}+B_{12}-[B_{13}+B_{23}]\right)^2=0 \quad (6)$$

For the ternary PMMA/PEMA/PVPh blends, a linear composition dependence of the interaction energy densities will be adopted for the miscible pairs ($B_{ij} = a_{ij} + b_{ij}\phi_i$; $i = 1, j = 2, 3$), to be consistent with our experimental data. Then the spinodal equation will be

$$\left(\frac{RT/V_1}{\phi_1}+\frac{RT/V_3}{\phi_3}-2B_{13}'+\phi_2\frac{\partial B_{12}'}{\partial\phi_1}+\phi_3\frac{\partial B_{13}'}{\partial\phi_1}\right)\times\left(\frac{RT/V_2}{\phi_2}+\frac{RT/V_3}{\phi_3}-2B_{23}\right)-\left(\frac{RT/V_3}{\phi_3}+B_{12}'-[B_{13}'+B_{23}]\right)^2=0 \quad (7)$$

where

$$B_{ij}' = B_{ij} + \phi_i\frac{\partial B_{ij}}{\partial\phi_i} \quad (8)$$

We note that if the dependence on composition of B_{12} and B_{13} is suppressed, eq 7 reduces to the classical spinodal equation for ternary systems (eq 6), as it should. Ternary miscibility boundaries are described by eqs 6 and 7 in terms of polymer molar volumes V_i and interaction energy densities B_{ij}.

The distinct miscibility gaps of ternary PMMA/PEMA/PVPh, PMMA/PEMA/PVF_2, and PMMA/PEMA/SAN blends provide a good test of the validity of the above theoretical approach exposed since all the B_{ij}'s between miscible pairs and molar volumes are available (see Table III), and, therefore, the same values of the interaction energy density between PMMA and PEMA (B_{23}) must be obtained from each ternary system. The assumed miscibility boundaries for the ternary diagrams are shown in Figures 11–13, and the results obtained from fitting eqs 6 and 7 at different PMMA/PEMA ratios are presented in Figure 14. A proper change of the miscibility limits between the blend compositions that show a single T_g or two T_g's provides an estimate of the uncertainty involved in this procedure, as shown in Figure 14 by error bars. Although B_{23} is assumed to be constant in eqs 6 and 7, the same dependence on composition of this parameter was obtained for each of the ternary systems studied here. The good agreement between the data derived from different ternary systems is encouraging and reflects the ability of the Flory–Huggins theory to model the miscibility behavior of this kind of system. The presence of immiscibility regions in the ternary diagram is explained by this theory as a consequence of different strengths of the interaction energies between components, even if favorable interactions are present.[12,35,36] In fact, the miscibility behavior of SAN/polycaprolactone (PCL)/SMA blends[37] has confirmed the theoretically predicted possibility of closed-loop miscibility gaps in ternary blends where all the binary pairs are miscible.

It appears that the above thermodynamic model provides a convenient framework for interpreting and designing miscibility behavior of ternary polymer blends. Quantitative information about binary interaction energies can be extracted from experimental ternary diagrams or, by the reverse procedure, a predicted diagram can be constructed when interaction energy values are available. As an example, Figure 15 illustrates the calculated miscibility boundary for PMMA/PEMA/SMA blends using the data from Figure 14 and Table IV. Future work is planned to confirm the predictive character of this theoretical approach.

Conclusions

The PMMA/PEMA/PVPh ternary diagram exhibits miscibility at relatively high percentages of PVPh (>60 wt %). DSC analysis has revealed the presence of two

Table III
Interaction Energy Densities B_{ij} and Polymer Molar Volumes V_i of Ternary Blends Involving the Immiscible PMMA/PEMA Pair

				$B_{ij} = a_{ij} + b_{ij}\phi_i$	
ternary system	polymer	V_i (cm³/mol)	i/j miscible pair	a_{ij} (cal/cm³)	b_{ij} (cal/cm³)
PMMA/PEMA/PVPh	PMMA	4.62×10^4	PVPh/PMMA	-10.53	-10.47
	PEMA	1.38×10^5	PVPh/PEMA	-11.96	-10.49
	PVPh	1.30×10^4			
PMMA/PEMA/PVF_2[a]	PMMA	3.13×10^4	PVF_2/PMMA	-2.98	
	PEMA	1.75×10^5	PVF_2/PEMA	-2.86	
	PVDF	1.23×10^5			
PMMA/PEMA/SAN[b]	PMMA	5.13×10^4	SAN/PMMA	-0.024[c]	
	PEMA	1.38×10^5	SAN/PEMA	-0.038[c]	
	SAN	1.85×10^3			

[a] Source: ref 5. [b] Source: ref 6. [c] Calculated from ref 19.

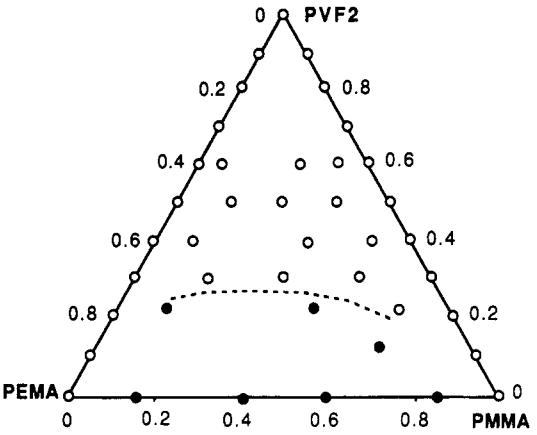

Figure 12. Ternary diagram of the PMMA/PEMA/PVF_2 system.[5] The open circles represent compositions where a single T_g is observed, and the full circles represent compositions where two glass transitions are observed. The miscibility boundary is denoted by the broken line. (Coordinates in volume fraction.)

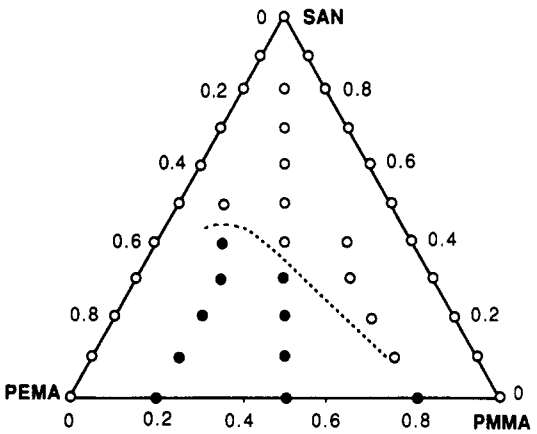

Figure 13. Ternary diagram of the PMMA/PEMA/SAN system.[6] The open circles represent compositions where a single T_g is observed, and the full circles represent compositions where two glass transitions are observed. The miscibility boundary is denoted by the broken line. (Coordinates in volume fraction.)

phases in the immiscible region of this diagram, in agreement with SEM results. By comparing PVPh, PVF_2, and SAN as compatibilizers for PMMA/PEMA immiscible blends, SAN and PVF_2 were found to be more effective than PVPh. The Flory–Huggins theory extended to ternary polymer blends provides a satisfactory explanation of this experimental trend. A knowledge of interaction parameters for the miscible pairs in ternary PMMA/PEMA/PVPh, PMMA/PEMA/PVF_2, and PMMA/PEMA/SAN blends has allowed us to obtain the interaction

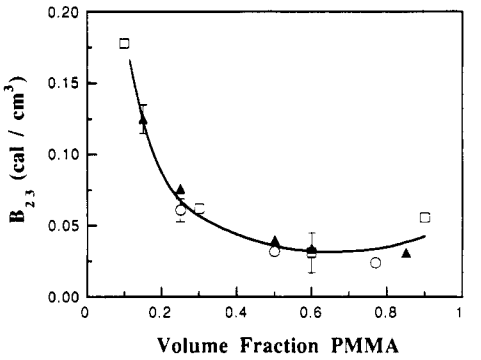

Figure 14. Interaction energy density between PMMA and PEMA derived from miscibility boundaries of several ternary systems: (□) PMMA/PEMA/PVPh; (▲) PMMA/PEMA/PVF_2; (○) PMMA/PEMA/SAN.

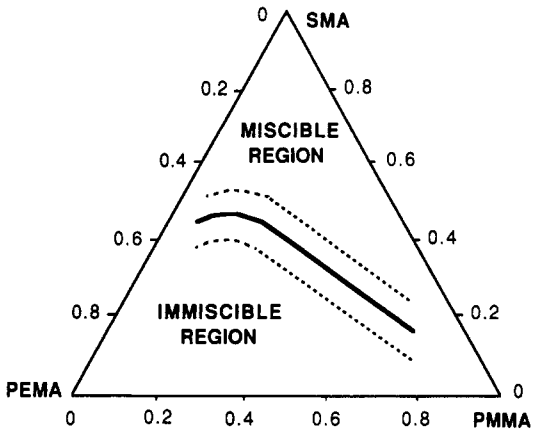

Figure 15. Estimated miscibility boundary for ternary PMMA/PEMA/SMA blends (see text).

Table IV
Interaction Energy Densities B_{ij} and Polymer Molar Volumes V_i of Ternary PMMA/PEMA/SMA Blends[a]

polymer	V_i (cm³/mol)	i/j miscible pair	B_{ij} (cal/cm³)
PMMA	4.62×10^4	SMA/PMMA	-0.26[b]
PEMA	1.38×10^5	SMA/PEMA	-0.27[b]
SMA	8.18×10^4		

[a] A copolymer containing 14 wt % maleic anhydride and M_n = 90 000 was considered. [b] Calculated from ref 19.

energy B_{23} between PMMA and PEMA. B_{23} values derived from each system correlate quite well, showing a composition dependence between the limits of previously reported data. A prediction of miscibility behavior for ternary PMMA/PEMA/SMA blends was attempted based on these values.

Acknowledgment. Financial support of this work by UPV/EHU (Project No. 203215-EB096/92) is gratefully acknowledged.

References and Notes

(1) Harris, J. E.; Goh, S. H.; Paul, D. R.; Barlow, J. W. *J. Appl. Polym. Sci.* **1982**, *27*, 839.
(2) Moskala, E. J.; Varnell, D. F.; Coleman, M. M. *Polymer* **1985**, *26*, 228.
(3) Goh, S. H.; Siow, K. S. *Polym. Bull.* **1987**, *17*, 453.
(4) Serman, G. J.; Xu, J.; Painter, P. C.; Coleman, M. M. *Macromolecules* **1989**, *22*, 2015.
(5) Kwei, T. K.; Frisch, H. L.; Radigan, W.; Vogel, S. *Macromolecules* **1977**, *10*, 157.
(6) Goh, S. H.; Siow, K. S. *Thermochim. Acta* **1986**, *105*, 191.
(7) Goh, S. H.; Siow, K. S.; Yap, K. S. *Thermochim. Acta* **1986**, *102*, 281.
(8) Christiansen, W. H.; Paul, D. R.; Barlow, J. W. *J. Appl. Polym. Sci.* **1987**, *34*, 537.
(9) Ameduri, B.; Prud'homme, R. E. *Polymer* **1988**, *29*, 1052.
(10) Koklas, S. N.; Sotiropoulou, D. D.; Kallitsis, J. K.; Kalfoglou, N. K. *Polymer* **1991**, *32*, 66.
(11) Landry, C. J. T.; Yang, H.; Machell, J. S. *Polymer* **1991**, *32*, 44.
(12) Su, A. C.; Fried, J. R. *Polym. Eng. Sci.* **1987**, *27*, 1657.
(13) Brannock, G. R.; Paul, D. R. *Macromolecules* **1990**, *23*, 5240.
(14) Flory, P. J. *Principles of Polymer Chemistry*; Cornell University Press: Ithaca, NY, 1953.
(15) Quian, C.; Mumby, S. J.; Eichinger, B. E. *Macromolecules* **1991**, *24*, 1655.
(16) Van Krevelen, D. W. *Properties of Polymers*; Elsevier Scientific Publishing Co.: Amsterdam, 1976.
(17) Luengo, G.; Rojo, G.; Rubio, R. G.; Prolongo, M. G.; Masegosa, R. M. *Macromolecules* **1991**, *24*, 1315.
(18) Temblay, C.; Prud'homme, R. E. *J. Polym. Sci., Polym. Phys. Ed.* **1984**, *22*, 1857.
(19) Brannock, G. R.; Barlow, J. W.; Paul, D. R. *J. Polym. Sci., Polym. Phys. Ed.* **1991**, *29*, 413.
(20) Nishimoto, M.; Keskkula, H.; Paul, D. R. *Macromolecules* **1990**, *23*, 3633.
(21) Pomposo, J. A.; Eguiazabal, I.; Calahorra, E.; Cortazar, M. *Polymer* **1993**, *34*, 95.
(22) Bernstein, R. E.; Cruz, C. A.; Paul, D. R.; Barlow, J. W. *Macromolecules* **1977**, *10*, 581.
(23) Walsh, D. J.; Cheng, G. L. *Polymer* **1984**, *25*, 499.
(24) Rodgers, P. A.; Paul, D. R.; Barlow, J. W. *Macromolecules* **1991**, *24*, 4101.
(25) Landry, C. J. T.; Teegarden, D. M. *Macromolecules* **1991**, *24*, 4310.
(26) Paul, D. R.; Barlow, J. W.; Keskkula, H. *Encyclopedia of Polymer Science and Engineering*, 2nd ed.; Mark, H. F., Bikales, N. M., Overberger, C. G., Menges, G., Eds.; John Wiley: New York, 1988; Vol. 12, p 399.
(27) Lai, C. H.; Paul, D. R.; Barlow, J. W. *Macromolecules* **1989**, *22*, 374.
(28) Machado, J. M.; French, R. N. *Polymer* **1992**, *33*, 760.
(29) Fernandes, J. H.; Barlow, J. W.; Paul, D. R. *J. Appl. Polym. Sci.* **1986**, *32*, 5481.
(30) Utracki, L. A.; Weiss, R. A., Eds. *Multiphase Polymers: Blends and Ionomers*; American Chemical Society: Washington, DC, 1989.
(31) Kwei, T. K.; Patterson, G. D.; Wang, H. H. *Macromolecules* **1976**, *5*, 780.
(32) Kim, C. K.; Paul, D. R. *Macromolecules* **1992**, *25*, 3097.
(33) Scott, R. L. *J. Chem. Phys.* **1949**, *17*, 279.
(34) Tompa, H. *Trans. Faraday Soc.* **1949**, *45*, 1142.
(35) Zeman, L.; Patterson, D. *Macromolecules* **1972**, *5*, 513.
(36) Hellmann, E. H.; Hellmann, G. P.; Rennie, A. R. *Colloid Polym. Sci.* **1991**, *269*, 343.
(37) Defieuw, G.; Groeninckx, G.; Reynaers, H. *Contemp. Top. Polym. Sci.* **1989**, *6*, 423.